

Preparation and properties of triple perovskite $\text{La}_{3-3x}\text{Ca}_{1+3x}\text{Mn}_3\text{O}_{10}$ ferromagnetic thin films

H. Asano,^{a)} J. Hayakawa, and M. Matsui

Department of Materials Science and Engineering, Nagoya University, Furo-cho, Chikusa-ku, Nagoya, 464-01, Japan

(Received 7 April 1997; accepted for publication 5 June 1997)

The ferromagnetic compound $\text{La}_{3-3x}\text{Ca}_{1+3x}\text{Mn}_3\text{O}_{10}$ with a triple perovskite structure can be successfully synthesized by using a thin-film growth method. Sputtered *a*-axis thin films with $x = 0.3$ have been examined with respect to their magnetotransport properties. For the triple perovskite compound, we have observed the features, including the enhanced magnetoresistance (MR) effect and the characteristic low-temperature MR effect resulting from intragrain spin-polarized tunneling, which were reported for the double perovskite manganites. A comparison of the magnitude of these features in triple and double perovskite manganites suggests that the features are actually determined by the *c*-axis Mn–O bond configuration in a layered-perovskite ferromagnet. © 1997 American Institute of Physics. [S0003-6951(97)01832-9]

The colossal magnetoresistance (CMR) effect in rare-earth manganese perovskites has aroused considerable interest in scientific studies and potential technological applications. The magnetic and electronic properties of the cubic (or pseudocubic) perovskites $\text{Ln}_{1-x}\text{M}_x\text{MnO}_3$ (Ln being rare-earth ions and M divalent cations), such as $\text{La}_{1-x}\text{Ca}_x\text{MnO}_3$ and $\text{La}_{1-x}\text{Sr}_x\text{MnO}_3$,¹⁻⁷ with three-dimensional Mn–O networks (isotropic MnO_6 octahedra), have been examined within the framework of the double exchange theory,^{8,9} which considers the transfer of an electron between neighboring Mn^{3+} and Mn^{4+} ions through the Mn–O–Mn path. However, recent theoretical and experimental studies¹⁰⁻¹³ have suggested that, in addition to the double exchange theory, some other effects, such as those relating to static or dynamic lattice distortions of the MnO_6 octahedra, are needed to understand the interplay between the carrier transport and the spin arrangement. Although studies have shown that the microstructure of the Mn–O network plays a crucial role with respect to the CMR effect, the exact role of the Mn–O microstructural networks in CMR perovskites remains unclear.

Recent studies have investigated the effect of the dimensionality of the Mn–O networks on the magnetic and transport properties in CMR perovskites through the use of several sample forms of double perovskite compounds of $(\text{La}-\text{M})_3\text{Mn}_2\text{O}_7$ (M = Sr, Ca).¹⁴⁻¹⁹ It has been reported that double perovskite manganites exhibit remarkable features including magnetoresistance (MR) ratio enhancement, anisotropic transport in charge carriers, existence of two types of ferromagnetic exchanges, a possible two-dimensional spin configuration, and the characteristic low-temperature MR effect resulting from intragrain spin-polarized tunneling. All these features could be essentially related to the series of alternating Mn–O–Mn and Mn–O–O–Mn bonds in the *c*-axis (out-of-plane) direction. Since the double perovskite compound of $(\text{La}-\text{M})_3\text{Mn}_2\text{O}_7$ is a member ($n=2$) of the Ruddlesden–Popper phases^{20,21} having the generic formula $\text{A}_{n+1}\text{B}_n\text{O}_{3n+1}$, the Mn–O bond configuration in the *c*-axis

direction, therefore, the degree of dimensionality can be modified by the use of higher-order ($n>2$) compounds. With a view to a further and quantitative understanding of the effect of dimensionality on these features, it is of fundamental importance to prepare layered-perovskite compounds with higher-order polytypes. However, this is expected to be difficult to achieve using bulk processes, because the intergrowth of other order polytypes can occur in $\text{A}_{n+1}\text{Ti}_n\text{O}_{3n+1}$ (A = Ca, Sr).^{20,21}

In this letter, we report results on the successful preparation of the triple perovskite ($n=3$) compound $\text{La}_{3-3x}\text{Ca}_{1+3x}\text{Mn}_3\text{O}_{10}$ by means of a thin-film technique. We examined the magnetic and transport properties of the sputtered *a*-axis thin films with $x = 0.3$. We found that the several remarkable features reported for double perovskite manganites can also exist in the triple perovskite compound. A comparison of the magnitude of these features for the triple and double perovskite manganites indicated that the Mn–O bond configuration in the *c*-axis direction determines these features in a layered-perovskite ferromagnet.

In the early stages of this work, we tried to prepare bulk samples of the triple perovskite ($n=3$) compound by using a conventional bulk ceramic process under several different conditions. Although we prepared the samples with a composition of $\text{La}_{3-3x}\text{Ca}_{1+3x}\text{Mn}_3\text{O}_y$, all the bulk samples contained a large proportion ($>80\%$) of the double perovskite compound. We then moved on to sample preparation using a thin-film method of a single-target magnetron sputtering technique. The sputtering conditions we employed here were almost identical to those used for thin films of $\text{La}_{2-2x}\text{Ca}_{1+2x}\text{Mn}_2\text{O}_7$, except for the target material (composition). Targets were 70 mm ϕ disks with a nominal composition $(\text{La}_{2.1}\text{Ca}_{1.9}\text{Mn}_3\text{O}_y)$. The target materials themselves consisted of a mixture of double and triple perovskite phases. Thin films 100–200 nm thick were grown on MgO (001) substrates whose temperatures were in the 700–750 °C range. Compositional analyses were performed using energy dispersive x-ray microanalysis (EDX), which indicated that the compositions of the obtained films were nearly identical to the nominal one within the accuracy ($\sim 2\%$) of EDX.

^{a)}Electronic mail: asano@numse.nagoya-u.ac.jp

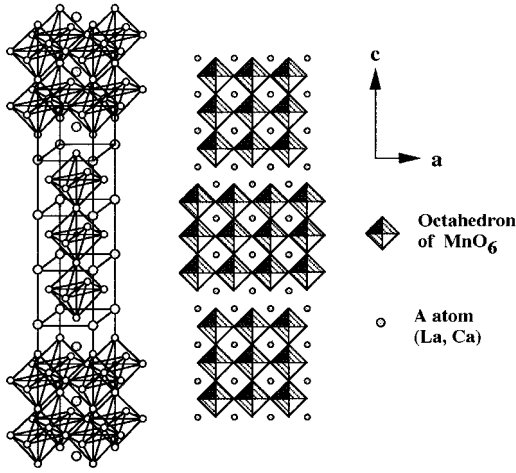


FIG. 1. Crystal structure and layer sequence of triple perovskite $\text{La}_{3-3x}\text{Ca}_{1+3x}\text{Mn}_3\text{O}_{10}$.

Film orientation in both the out-of-plane and in-plane directions, phase identification, and lattice parameters were determined using x-ray diffraction analysis with a four-axis goniometer. In the diffraction spectra of thin films grown on MgO (100) under the above deposition conditions, only ($L00$) reflections were present, indicating that the films grew with their a -axis normal to the substrate surface. Fourfold symmetry was revealed from ϕ -scan (in-plane rotation) analysis, indicating that the a -axis films were ordered in the plane and consisted of two domains, rotated at 90° to each other, in the film plane. These diffraction data gave us lattice parameters a_0 , c_0 , and c_0/a_0 of 0.3867 nm, 2.680 nm, and 6.930, respectively. This c_0/a_0 value indicates that the phase of the thin films is a triple ($n=3$) perovskite, whose crystal structure is shown in Fig. 1.

To our knowledge, nothing has been published to date on the phase stability of compound $(\text{La-Ca})_{n+1}\text{Mn}_n\text{O}_{3n+1}$ with $n=3, 4$, etc. Our preliminary results reveal that samples prepared by a bulk sintering method contained a large proportion of the double ($n=2$) perovskite compound in coexistence with a very small amount of the triple perovskite ($n=3$) compound, even when the samples were prepared with a composition of $\text{La}_{3-3x}\text{Ca}_{1+3x}\text{Mn}_3\text{O}_y$. It is our belief that the problem of phase stability is sufficiently severe that the single phase $n=3$ compound cannot be prepared by bulk preparation methods. However, this compound can be prepared by a thin-film growth method. The conditions for the formation of the $n=3$ compound by a thin-film method differ in at least two essential aspects from formation by a bulk method. First, the growth temperature of the thin film is low ($\sim 700^\circ\text{C}$) compared to the bulk formation temperature. Second, the geometry of the deposition process is different from the bulk geometry of the sintering process. These factors might be favorable in terms of stabilizing the single phase $n=3$ compound, although the precise mechanism for stabilizing the triple perovskite phase using a thin-film method is unclear at present.

The electrical resistivity was measured as a function of temperature and magnetic field using the standard four-point technique. The field was applied parallel to the film surface. In Fig. 2, we show the temperature dependence of the resistivity ρ under various magnetic fields for a thin film of $\text{La}_{3-3x}\text{Ca}_{1+3x}\text{Mn}_3\text{O}_{10}$ ($x=0.3$).

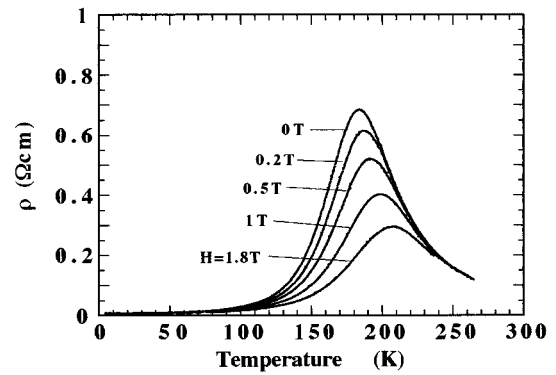


FIG. 2. Temperature dependence of resistivity ρ for a thin film of $\text{La}_{3-3x}\text{Ca}_{1+3x}\text{Mn}_3\text{O}_{10}$ ($x=0.3$) under various magnetic fields.

Figure 2 shows the temperature dependence of resistivity ρ under various magnetic fields for a thin film of $\text{La}_{3-3x}\text{Ca}_{1+3x}\text{Mn}_3\text{O}_{10}$. In the zero field, there is a peak in the ρ - T curve at 184 K with metallic behavior below and semiconducting behavior above this temperature. Hereafter, the peak temperature in resistivity is referred to as T_ρ^{max} . The T_ρ^{max} value of the $\text{La}_{3-3x}\text{Ca}_{1+3x}\text{Mn}_3\text{O}_{10}$ (184 K) falls between the values reported for $\text{La}_{2-2x}\text{Ca}_{1+2x}\text{Mn}_2\text{O}_7$ (133–140 K) and $\text{La}_{1-x}\text{Ca}_x\text{MnO}_3$ (230–240 K) with an identical carrier concentration ($x=0.3$). The resistivity ρ of the thin film at 4.2 K is 8 m Ω cm. This ρ value for $\text{La}_{3-3x}\text{Ca}_{1+3x}\text{Mn}_3\text{O}_{10}$ also falls between the values we previously reported for $\text{La}_{2-2x}\text{Ca}_{1+2x}\text{Mn}_2\text{O}_7$ (30 m Ω cm) and $\text{La}_{1-x}\text{Ca}_x\text{MnO}_3$ (0.3 m Ω cm) thin films with an identical carrier concentration ($x=0.3$).

The temperature dependence of the MR ratio $-\Delta\rho/\rho_0$ for $\text{La}_{3-3x}\text{Ca}_{1+3x}\text{Mn}_3\text{O}_{10}$ thin film is derived from the data in Fig. 2, and is shown in Fig. 3. The MR ratio is defined as $-\Delta\rho/\rho_0 = -(\rho_{1T} - \rho_0)/\rho_0$ (where ρ_{1T} and ρ_0 are the resistivity in an applied magnetic field of 1 T and the zero-field resistivity, respectively). The MR effect is observed over a wide temperature range from a low temperature to ~ 240 K. In the MR- T curve, the MR shows a maximum near T_ρ^{max} , and the maximum MR ratio is 61%. When this maximum MR ratio is compared with our thin-film data for $\text{La}_{2-2x}\text{Ca}_{1+2x}\text{Mn}_2\text{O}_7$ and $\text{La}_{1-x}\text{Ca}_x\text{MnO}_3$ with an identical carrier concentration ($x=0.3$), this value lies between those (93% and 50%) for $\text{La}_{2-2x}\text{Ca}_{1+2x}\text{Mn}_2\text{O}_7$ and

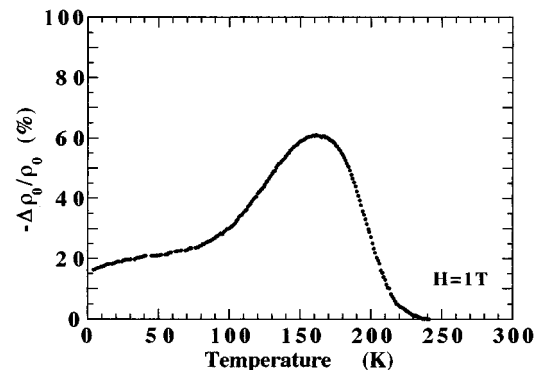


FIG. 3. Temperature dependence of the MR ratio ($-\Delta\rho/\rho_0$) in $H=1$ T for a thin film of $\text{La}_{3-3x}\text{Ca}_{1+3x}\text{Mn}_3\text{O}_{10}$ ($x=0.3$). The MR ratio is calculated from the data in Fig. 2.

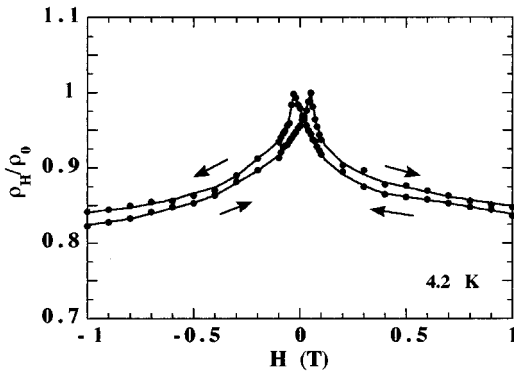


FIG. 4. Normalized resistivity ρ_H/ρ_0 and magnetization as a function of applied magnetic field at 4.2 K for a thin film of $\text{La}_{3-3x}\text{Ca}_{1+3x}\text{Mn}_3\text{O}_{10}$ ($x=0.3$). These data were obtained after an initial application of a magnetic field of +1.8 T, and sampling cycles are shown as arrows. The solid lines are drawn only as a guide to the eyes.

$\text{La}_{1-x}\text{Ca}_x\text{MnO}_3$, respectively. The MR shows a relatively sharp decrease with decreasing temperatures to ~ 80 K, and displays a gradual decrease with decreasing temperatures down to 4.2 K. At 4.2 K, the MR ratio is 16%, which is much smaller than that for the $\text{La}_{2-2x}\text{Ca}_{1+2x}\text{Mn}_2\text{O}_7$ thin film (50%).¹⁷ It is noteworthy that $\text{La}_{1-x}\text{Ca}_x\text{MnO}_3$ thin films do not exhibit the MR effect in this low-temperature range. To obtain further insight into the low-temperature MR effect, we examined the field dependence of normalized resistivity and magnetization for thin-film $\text{La}_{3-3x}\text{Ca}_{1+3x}\text{Mn}_3\text{O}_{10}$ at 4.2 K and the results are shown in Fig. 4. Apparent hysteresis can be seen in the resistivity versus magnetic-field curve at 4.2 K. We found that the magnetic fields, which led to the resistivity peak in the MR- H curve correspond to the fields at which zero magnetization is obtained in the magnetization-magnetic field ($M-H$) curve (not shown). This feature of the $\text{La}_{3-3x}\text{Ca}_{1+3x}\text{Mn}_3\text{O}_{10}$ thin film is believed to be due primarily to the spin-polarized tunneling effects in the ferromagnet/insulator/ferromagnet structure.

The features observed here are, in principle, similar to those for $\text{La}_{2-2x}\text{Ca}_{1+2x}\text{Mn}_2\text{O}_7$ thin films. Moreover, it should be mentioned that the magnet behavior for the present films (not shown here) is similar to that for the $\text{La}_{2-2x}\text{Ca}_{1+2x}\text{Mn}_2\text{O}_7$ thin films,¹⁷ which indicates the existence of the two types of ferromagnetic exchanges. We can interpret these features as being the essential results of anisotropic hole transfer and exchange interaction. We suggest that the lower critical temperature, T_ρ^{max} , is related to the exchange interaction in the c -axis direction. Based on our hypothesis, it is interesting to compare the thin-film data for $n=2$ and 3 with an identical carrier concentration ($x=0.3$). The fact that T_ρ^{max} for the $n=3$ compound is larger than that for the $n=2$ compound indicates that the c -axis exchange interaction for the $n=3$ compound is stronger than that for the $n=2$ compound. It is reasonable to believe that there is a stronger c -axis exchange interaction in the $n=3$ compound than in the $n=2$ compound, since the (positive) double exchange interaction in the Mn-O-Mn-O-Mn bond (triple perovskite layer) is stronger than that in the Mn-O-O-Mn bond (double perovskite layer). Moreover, it is noteworthy that the magnitude of the MR effects can also be

interpreted in terms of the c -axis exchange interaction. The MR effect near T_ρ^{max} can be explained by the spin dependent electron hopping mechanism predicted by the double exchange models. In these models, it is evident that a stronger exchange interaction can cause an enhanced effective transfer interaction in the charge carriers, which results in a lowering of the MR ratio via the weakened effective coupling between the local spin and the charge carrier. In contrast, the low-temperature MR effect can be understood by the intragrain (intrinsic) spin-polarized tunneling through the insulating Mn-O-O-Mn bond. The large difference between the MR ratios (at 4.2 K) for the $n=3$ (16%) and $n=2$ (50%) thin film suggests that the transfer interaction in the c -axis direction has considerable influence on the low-temperature MR effect.

In conclusion, we have succeeded in preparing a triple perovskite ($n=3$) compound $\text{La}_{3-3x}\text{Ca}_{1+3x}\text{Mn}_3\text{O}_{10}$ by means of a thin-film technique. We found that the features reported for the double perovskite manganites also exist in triple perovskite manganites. It is apparent from the trends observed in the $(\text{La-Ca})_{n+1}\text{Mn}_n\text{O}_{3n+1}$ series compounds that there is a clear correlation between the dimensionality (or the c -axis bond configuration) and the magnetotransport properties. Further studies are necessary to obtain a unified interpretation of the relationships between the dimensionality and the electronic and magnetic properties for the series compounds.

¹R. von Helmolt, J. Wecker, B. Holzapfel, L. Schultz, and K. Samwer, Phys. Rev. Lett. **71**, 2331 (1993).

²K. Chahara, T. Ohno, M. Kasai, and Y. Kozono, Appl. Phys. Lett. **63**, 1990 (1993).

³Y. Tokura, A. Urushibara, Y. Moritomo, T. Arima, A. Asamitsu, G. Kido, and N. Furukawa, J. Phys. Soc. Jpn. **63**, 3931 (1994).

⁴H. L. Ju, C. Kwon, Qi Li, R. L. Greene, and T. Venkatesan, Appl. Phys. Lett. **65**, 2117 (1994).

⁵S. Jin, H. M. O'Bryan, T. H. Tiefel, M. McCormack, and W. W. Rhodes, Appl. Phys. Lett. **66**, 382 (1995).

⁶P. Schiffer, A. P. Ramirez, W. Bao, and S. W. Cheong, Phys. Rev. Lett. **75**, 3336 (1995).

⁷H. Y. Hwang, S. W. Cheong, P. G. Radaelli, M. Marezio, and B. Batlogg, Phys. Rev. Lett. **75**, 914 (1996).

⁸C. Zener, Phys. Rev. **82**, 403 (1951).

⁹P. G. de Gennes, Phys. Rev. **118**, 141 (1960).

¹⁰A. J. Millis, P. B. Littlewood, and B. I. Shraiman, Phys. Rev. Lett. **74**, 5144 (1995).

¹¹H. Roder, J. Zang, and A. R. Bishop, Phys. Rev. Lett. **76**, 1356 (1996).

¹²G. Zhao, K. Conder, H. Keller, and K. A. Muller, Nature (London) **381**, 676 (1996).

¹³A. Shengelaya, G. Zhao, H. Keller, and K. A. Muller, Phys. Rev. Lett. **76**, 5296 (1996).

¹⁴Y. Moritomo, Y. Tomioka, A. Asamitsu, Y. Tokura, and Y. Matsui, Nature (London) **380**, 141 (1996).

¹⁵H. Asano, J. Hayakawa, and M. Matsui, Appl. Phys. Lett. **68**, 3638 (1996).

¹⁶H. Asano, J. Hayakawa, and M. Matsui, Jpn. J. Appl. Phys., Part 2 **36**, L104 (1997).

¹⁷H. Asano, J. Hayakawa, and M. Matsui, Appl. Phys. Lett. **70**, 2303 (1997).

¹⁸T. Kimura, Y. Tomioka, H. Kuwahara, A. Asamitsu, M. Tamura, and Y. Tokura, Science **274**, 1698 (1996).

¹⁹R. Suryanarayanan, I. Zelenay, and J. Berthon, Mat. Res. Bull. **32**, 595 (1997).

²⁰S. N. Ruddlesden and P. Popper, Acta Crystallogr. **11**, 54 (1958).

²¹M. M. Elcombe, E. H. Kisi, K. D. Wawkins, T. J. White, P. Goodman, and S. Matheon, Acta Crystallogr. Sec. B **47**, 305 (1958).